JOURNAL OF CATALYSIS **162,** 198–208 (1996)
ARTICLE NO. 0277

Hydroconversion of Heptane over Pt/Al-Pillared Montmorillonites and Saponites

A Comparative Study

S. Moreno, R. Sun Kou, and G. Poncelet*

Unité de Catalyse, Université Catholique de Louvain, Place Croix du Sud 2/17, 1348 Louvain-la-Neuve, Belgium

Received October 26, 1995; revised April 10, 1996; accepted April 30, 1996

Montmorillonites and saponites have been pillared with oxo-hydroxy-aluminium solutions (OH/Al molar ratio of 1.6). The solids have been examined by X-ray diffraction. The textural properties, residual cation exchange capacities, and acid contents have been established. The pillared clays exhibit thermally stable spacings, specific surface areas, and micropore volumes typical of such materials. Higher acid contents were found for pillared saponites than for pillared montmorillonites. IR spectroscopy of pillared saponites showed a new OH stretching vibration at 3595 cm^{-1}, absent in pillared montmorillonites. The acid character of these OH groups has been assessed by pyridine adsorption. The catalytic properties have been evaluated over Pt-impregnated samples in the heptane hydroisomerisation reaction. Al-pillared saponites, smectites with lattice Si for Al tetrahedral substitutions, showed superior catalytic performances (high conversions, high yields of isomers) compared with Al-pillared montmorillonites, clays with lattice octahedral substitutions. The higher activity of the saponites is attributed to the higher content and strength of the acid sites associated with Si–OH . . . Al groups produced upon proton attack of the tetrahedral Si–O–Al bonds. Such strong acid sites are absent in Al-pillared montmorillonites.

INTRODUCTION

Pillared clays with different types of pillars have been described in the literature over the last 20 years. Al-pillared clays are by far the most documented ones and are nowadays easy to prepare in a reproducible way, probably because the chemistry of aluminium in solution is relatively better controlled compared with that of other metals. Moreover, these microporous acid solids have shown appealing catalytic aptitudes in a broad range of reactions involving organic molecules. Recently, Mokaya and Jones (1, 2) showed that the Brønsted acidity and the catalytic properties of Al-pillared montmorillonite could be improved by an acid activation of the clay prior to its pillaring.

* Author to whom correspondence should be addressed.

In previous work, the importance of the nature of the starting clay on the catalytic performances of its Al-pillared form has been demonstrated in several reactions. Indeed, evidence has been provided that Al-pillared beidellite, a clay with tetrahedral lattice Si for Al substitutions, was noticeably more active than Al-pillared montmorillonite (with Al for Mg substitutions in the octahedral layers) in proton-catalysed reactions (3–8). Recent results on the hydroisomerisation-hydrocracking of decane over Pt/Al-pillared clays prepared with a montmorillonite, a synthetic beidellite and two smectites with intermediate levels of tetrahedral substitutions, confirmed the superiority of beidellite over montmorillonite, the clays with partial beidellitic character showing catalytic performances proportional to the degree of tetrahedral substitutions (9). The higher activity of Al-pillared beidellite over Al-pillared montmorillonite, both prepared under identical conditions, was accounted for by the presence of stronger acid sites, as a result of the proton attack of tetrahedral Si–O–Al bonds and formation of Si–OH . . . Al acid sites. These bonds are almost nonexistent in montmorillonite and, hence, such strong sites are absent (10). Higher activity of pillared beidellite, compared with pillared montmorillonite, has also been observed by Butruille and Pinnavaia (11) in the alkylation of biphenyl with propylene as well as by Jiang *et al.* (12) who found a relationship between activity and tetrahedral Al in the hydroisomerisation of hexane.

It was of interest to examine whether other swelling clays with framework tetrahedral substitutions would develop, upon Al-pillaring, microporous materials with catalytic performances close to those obtained over Al-pillared beidellite. Saponite, a magnesian swelling clay with tetrahedral Al for Si substitutions, was a good candidate. Al-pillared saponites have been recently prepared and thoroughly characterised by Schoonheydt *et al.* (13), Chevalier *et al.* (14, 15), and Lambert *et al.* (16), and their catalytic properties in the cracking of heavy petroleum feedstock were compared with those of a commercial FCC catalyst (17).

0021-9517/96 $18.00

In this study, Al-pillared saponites and montmorillonites have been prepared and characterised, and their catalytic behavior has been investigated in the hydroisomerisation–hydrocracking of heptane over Pt-impregnated samples.

EXPERIMENTAL

Materials

Four swelling clays from different deposits were selected for this study:

— a montmorillonite from Chile (W-140 P), with trade name Minclay supplied by Deltamat-Paquet, Belgium
— a Spanish montmorillonite (SB), Serrata Blanca
— two saponites from Spanish deposits, Vicalvaro (SC-27) and Esmectita de Yunclillos (EY) provided by Tolsa, Madrid.

In addition, the Ballarat saponite (SAPCA), with good crystallinity, supplied by Source Clay Minerals Repository, Univ. of Missouri, Columbia, U.S.A., was occasionally used for comparison purposes. This clay has been characterised by Post (18). X-ray diffraction spectra of the two montmorillonites did not show the presence of detectable amounts of other crystalline mineral phases, whereas the saponites (SC-27 and EY) were contaminated by sepiolite (about 20% and 10%, respectively).

Chemical analyses of the starting clays were performed by inductively coupled plasma spectroscopy (ICPS). The compositions are given in Table 1.

Pillaring Method

Pillaring experiments were done over both the raw (as received) clays and over the fractions smaller than 2 μm, separated by usual sedimentation methods. The pillaring procedure was similar to the one described in previous work (10). The pillaring solutions were prepared by the dropwise addition of 0.5 *M* NaOH solution to 0.2 *M* $Al(NO_3)_3$ solution, using the volume of the base necessary to reach an OH/Al molar ratio of 1.6 (for most preparations). After standing for 24 h at room temperature, the pillaring solution was slowly dropped into the clay suspension (usually 2 wt% of clay), the volume of solution being adjusted in order to supply 20 meq Al per gram of clay (raw and small fraction). The final suspension was aged at room temperature for 24 h. Pillaring of Ballarat saponite (SAPCA) was done with Al-chlorhydrol solution (from Reheis Chem. Co.). These operations were conducted under continuous stirring. Excess salts were eliminated, as in earlier work (10), by dialysis, the washing water being renewed until the conductivity was reduced to its initial value. The pillared material was then freeze-dried. This procedure was applied to the unrefined clays as well as to the ≤ 2 μm fractions.

Characterisation Methods

X-ray diffraction spectra were recorded with a D-5000 Siemens instrument using a Cu anticathode, on samples dried at room temperature and after calcining separate samples for 2 h at different temperatures. The oriented film preparation method onto glass slides was adopted. The change of the *d* spacing (001 reflection) versus calcination temperature provides a direct appreciation of the thermal resistance of the intercalated pillars, while the half-height width of the 001 reflection yields qualitative information on the quality of the pillars (13, 19). As pillaring is the result of an exchange process between interlayer cations (Na^+) ensuring electroneutrality of the clay framework and positively charged pillar precursors (AlOH species) and the fact that all the exchange positions cannot, due to steric or size effects, be occupied by pillars, the measure of the number of sites which are not exchanged by AlOH species (residual CEC) gives an indication of the extent of pillaring. The initial and residual CECs have been determined by the micro-Kjeldahl method on samples previously treated with a 2 *M* ammonium acetate solution and washed free of excess salt.

The acid content of the pillared samples was determined by isothermic adsorption (IA) of ammonia followed by temperature programmed desorption (TPD). The following procedure was used: 200 mg of pillared material were treated in a U-shaped fixed-bed reactor for 2 h at 400°C under a flow of helium (60 ml/min), the free volume of the reactor on both sides of the sample being filled with

TABLE 1

Chemical Composition of the Starting Clays (wt%)

Clay	SiO_2	Al_2O_3	Fe_2O_3	MgO	TiO_2	CaO	Na_2O	K_2O	MnO
W140	73.94	14.55	1.92	3.29	0.33	0.22	1.68	0.11	0.026
SB	63.31	19.95	3.43	4.26	0.13	0.24	3.00	0.58	0.026
SC27[a]	48.87	5.03	1.52	24.09	0.20	1.80	0.19	1.00	—
EY	55.29	5.40	1.43	25.23	0.15	0.41	0.75	0.30	0.026
SAPCA	49.11	4.24	0.84	26.86	0.05	0.18	2.09	0.03	0.020

[a] Determined on the raw clay.

small-sized quartz (anal. grade). At the end of the pretreatment, the temperature was lowered to 250°C and stabilised by means of a temperature controller. Successive pulses of pure ammonia were then injected over the solid by means of a 6-way sampling valve provided with a loop of known volume. The evolution of the concentration of ammonia in the effluent was followed with a thermal conductivity detector, and the exit gas mixture at the outlet of the TCD cell was bubbled in a vessel containing 0.1 *M* boric acid. After saturation of the solid with ammonia, the total ammonia "trapped" by boric acid was back-titrated with diluted sulfuric acid. Knowing the number of pulses of ammonia and the amount injected per pulse, the quantity taken up by the solid was obtained by difference. The installation was then purged with a stream of helium. The reactor temperature was linearly increased up to 400°C at a rate of 10°C/min under a stream of helium, and the final temperature was maintained for 14 h. The TCD signal recorded during the desorption step was integrated, and the total amount of ammonia evolved and collected in boric acid was back-titrated. Using this procedure, the amount of ammonia adsorbed (or desorbed) by the solid corresponds to the acid content and, principally, to the proton content. Indeed, at 250°C, ammonia is adsorbed on the stronger acid sites which are of interest in catalysis. It will thus be assumed that each mmole of ammonia corresponds to one mmole of proton.

The textural characteristics (surface areas and micropore volumes) were obtained from nitrogen adsorption isotherms established at liquid nitrogen temperature, using an ASAP 2000 sorptometer from Micromeritics. The samples (2 μ fractions) were outgassed for 4 h at 200°C, without and with a precalcination step under air at 400°C for 2 h. The external surface areas and micropore volumes were established according to a method proposed by Remy and Poncelet (20).

Infrared spectroscopy has been used to investigate the OH stretching region of unpillared and pillared clays and to examine the spectral modifications occurring upon pyridine adsorption. This base, indeed, gives rise to specific absorption bands according to whether it interacts with Lewis or Brønsted acid sites. Thin films of clays were prepared by room temperature drying of clay suspensions deposited on Mylar sheets. The autocoherent films were then introduced in an IR cell which was connected to a glass apparatus provided with the necessary pumping and heating systems. Three clays (unpillared and pillared forms, 2 μ fractions) were examined, namely the reference saponite (SAPCA), the Spanish EY saponite, and the Serrata Blanca (SB) montmorillonite. The spectra were recorded with a FTIR (Bruker IFS-88) instrument after outgassing the samples for 14 h at 250°C under a residual pressure lower than 10^{-5} Torr. Pyridine was then adsorbed at room temperature for 30 min. Spectra were recorded after outgassing at room temperature for 1 h and at increasing temperatures for 2 h.

Catalytic Evaluation

The catalytic performances of the different Al-pillared clays have been evaluated in the hydroisomerisation-hydrocracking of heptane over samples previously impregnated with platinum tetrammine chloride solution (wet impregnation), using the required volume of solution to load the solids with 1 wt% of metal. The catalytic tests were performed in a fixed bed microreactor operated at atmospheric pressure. Activation of the catalyst was carried out as follows: The reactor containing the catalyst sandwiched between two layers of pure small sized quartz was heated at 400°C at a heating rate of 7°C/min under a flow of dry air and maintained at the final temperature for 2 h. The circuit was then purged with helium. The metal was reduced by flowing pure hydrogen through the catalyst bed for 2 h at 400°C. After this activation step, the reactor was cooled to 150°C and stabilised at this temperature. A stream of hydrogen saturated with heptane vapour was generated by passing hydrogen through a thermostated glass saturator filled with heptane and kept at constant temperature (27°C). The total flow (hydrogen-heptane) was 10 ml/min, and the WHSV was 0.9 g heptane/g catalyst.h. The reaction was carried out in temperature-programmed mode between 150 and 400°C, at a heating rate of 1.5°C/min. On-line gas phase analysis was performed in a HP-5880 gas chromatograph equipped with a 50 m capillary CPSil-5 column (from Chrompack) and FID. The temperature of the column was maintained at 30°C during the separation of the products.

The conversion percentages and yields were established on the basis of the carbon balance established from the chromatographic analyses, using the following method: The products of the peak areas of the different compounds and the FID sensitivity factors (21) were multiplied by the number of carbon atoms of each constituent detected in the reaction gas mixture (between 1, for methane, and 7, for heptane and isomers, and toluene). Heavier products, indeed, are absent under the experimental conditions adopted. Summing up these values yields the total quantity of carbon atoms (Q) identified in each analysis. This quantity corresponds to 100%. The yields of each family of products (isomers, cracked, and cyclic products) were obtained from the partial summations reported to 10^{-2}. Q, and the conversion percentages were given by the sum of the partial summations of each product family divided by 10^{-2}. Q. Within each family, the product distribution was established similarly on the basis of the partial summations.

For comparison purposes, the catalytic data obtained under strictly identical reaction conditions over other Al-pillared clays and acid zeolites, all being loaded also with 1 wt% Pt, have been compiled in the discussion section. The clays include a commercial montmorillonite (Westone L, AlP-W), two nickel- and iron-containing clays with different levels of tetrahedral substitutions, from Niquelandia

deposit, Brazil (AlP-N4 and AlP-N7), an Al-pillared synthetic beidellite (AlP-B), and two batch-prepared pillared clays (Zenith montmorillonite), AZA (Al-pillared) and FAZA (with Al-Fe mixed pillars), provided by Straton Hi-Tec, Athens, and recently described by Kaloidas *et al*. (22). Details on the preparation, characterisation, and catalytic properties of AlP-W, AlP-N4, AlP-N7, and AlP-B may be found elsewhere (7, 9). Concerning the H-zeolites, H-Y 82 was a Union Carbide sample, with Si/Al = 5.1, and CBV 600 from P. Q. Corp. (Si/Al = 2.8). H-mordenite was a large-port sample from Tosoh Corp., Japan, dealuminated by a steaming treatment at 600°C, followed by acid leaching with 2 *M* HNO_3. The Si/Al ratio of this sample was 49 (23).

RESULTS

Characterisation of the Pillared Clays

The values of the *d* spacings (001 reflection) of the pillared clays prepared with the $\leq 2\ \mu$ fractions and the raw clays are compared in Table 2. All the room temperature dried samples exhibit spacings above 18 Å, which progressively diminish as the calcination temperature increases. Still high values are observed after thermal treatment at 600°C. Using the raw clays or the $<2\ \mu$ fractions has no major effect on the spacings of the pillared forms. The values are generally similar to those expected for such materials.

The cation exchange capacity (CEC) values of the starting clays ($\leq 2\ \mu$ fractions) and of the pillared forms are indicated in Table 3. SB montmorillonite exhibits a high initial CEC. The lower values for SC27 and EY saponites reflect, at least partly, the contribution of contamination by sepiolite and, partly also, their poorer degree of crystallinity (stacking order) as inferred from the X-ray peak profile. A similar observation has been recently reported by Casal *et al*. (24) in the case of unpillared SC27.

As mentioned earlier, the peak width at half height yields information on the quality of the pillars and the stacking order (13, 19). Of course, lower values reflect better-ordered assemblies. The following half height widths were obtained from the X-ray recordings (400°C, 2 μ pillared clay fractions): 3.1, 3.7, 4.0, 5.5, and 6.3 Å for, respectively, AlP-SAPCA, AlP-SB, AlP-W140, AlP-EY, and AlP-SC27. Thus, going from AlP-SAPCA to AlP-SC27, there is a decreasing quality of the pillared materials. Schoonheydt *et al*. (13) found for a well-pillared saponite a value of 5 Å after calcination at 400°C.

Chemical analyses of the pillared materials were performed by ICPS in order to estimate the amount of Al involved in the pillars. Framework Al was distinguished from pillar Al using structural Mg as the internal reference. The values reported in Table 3 are noticeably lower than those obtained in previous studies (close to 2 mmol/g) (10); they are consistent with the relatively high residual CEC values.

The surface areas and micropore volumes of the Al-pillared samples ($\leq 2\ \mu$) obtained from the nitrogen adsorption isotherms of samples outgassed at 200°C for 4 h without and with a precalcination step at 400°C for 2 h are given in Table 4. High surface areas and micropore volumes are observed for the samples outgassed at 200°C. As expected, lower figures are obtained after a calcination at 400°C, and the loss of surface area is directly related to the decrease

TABLE 3

Initial and Residual CEC's, and the Amount of Pillar Al

Samples	CEC (mmol/g) $<2\ \mu$ fraction	CEC (mmol/g) crude clay	Al in pillar (mmol/g)
W140	0.811	—	—
AlP-W140	0.353	0.316	1.53
SB	1.10	—	—
AlP-SB	0.412	0.400	1.70
SC27	0.558	—	—
AlP-SC27	0.285	0.209	1.34
EY	0.612	—	—
AlP-EY	0.350	0.226	1.60

TABLE 2

X-Ray Diffraction Data: Basal Spacings (in Å) Observed after Calcination at Increasing Temperatures

Clay		Room temp.	200°C	400°C	600°C
AlP-W140	a	20.8	17.3	17.3	17.3
	b	18.8	18.4	17.3	17.0
AlP-SB	a	18.8	18.4	17.5	16.1
	b	19.2	19.6	18.8	17.0
AlP-SC27	a	18.4	17.7	17.0	16.1
	b	20.1	20.1	18.0	id
AlP-EY	a	18.2	17.3	17.0	16.7
	b	19.4	17.7	17.0	15.8
AlP-SAPCA	b	19.6	18.4	18.6	17.0

Note. a, $<2\ \mu$ fraction; b, raw clay; id, ill defined.

TABLE 4

Textural Characteristics of the Al-Pillared Clays

Clay		S_{BET} (m^2/g)	S_{BET} ext (m^2/g)	Micropore volume (cm^3/g)
AlP-W140	a	236	60	0.084
	b	175	60	0.055
AlP-SB	a	255	60	0.092
	b	243	62	0.086
AlP-SC27	a	293	134	0.076
	b	257	133	0.060
AlP-EY	a	300	100	0.095
	b	240	94.4	0.070
AlP-SAPCA	b	353	73.0	0.128

Note. a, uncalcined; b, calcined at 400°C for 2 h.

TABLE 5

Amounts of Ammonia Adsorbed at 250°C (IA) and Released under Temperature Programmed Conditions (TPD)

Pillared clay		IA (mmol/g)	TPD (mmol/g)
AlP-W140	a	0.130	0.111
	b	0.114	0.095
AlP-SB	a	0.165	0.148
	b	0.145	0.126
AlP-SC27	a	0.216	0.200
	b	0.208	0.200
AlP-EY	a	0.208	0.184
	b	0.213	0.191
AlP-SAPCA	b	0.298	0.275

Note. a, $<2\ \mu$ fraction; b, raw clay.

of microporosity. The pillared SB sample differs from the other pillared materials in its limited loss of textural properties upon calcination. It is also the sample which contains the highest amount of pillar Al and characterised by a low value of the half height peak width.

The amounts of ammonia adsorbed at 250°C (IA) and desorbed under temperature programmed conditions (TPD) are compared in Table 5. These values, as mentioned earlier, assume a 1 : 1 stoichiometry, namely each mmol NH_3 corresponds to one mmol of proton. The temperature of 250°C was adopted on the basis of poisoning experiments with ammonia carried out between 400 and 200°C. No reaction of heptane occurred up to a threshold of 250°C beyond which the reaction resumed.

As shown in Table 5, the IA and TPD results agree reasonably well, although the TPD values are slightly lower than the IA data. Nevertheless, both series of data show that Al-pillared saponites (SC27, EY, and SAPCA) have higher acid contents than Al-pillared montmorillonites (W140P and SB). Furthermore, pillaring the raw clays or the small fractions has no drastic influence on the acid contents, the discrepancies between pillared montmorillonites and saponites being maintained.

IR Spectroscopy

The IR spectra in the OH stretching vibration region of the unpillared and pillared clays are shown in Fig. 1. Unpillared saponites (SAPCA and EY) show a main absorption band near 3676–3677 cm^{-1}, which in montmorillonite occurs at around 3626 cm^{-1}. This main band, particularly narrow in saponites, is generally attributed to framework OHs (Mg_3OH units in saponites and Al_2OH units in montmorillonites). Saponites show, in addition, two broad and weakly intense bands centered near 3620 and 3520 cm^{-1}, the first one being associated with octahedral lattice substitutions. Chevalier *et al.* (15) noticed, in the case of SAPCA saponite, a small absorption between 3736 and 3716 cm^{-1}, barely distinguishable in our spectra (probably due to smaller weight

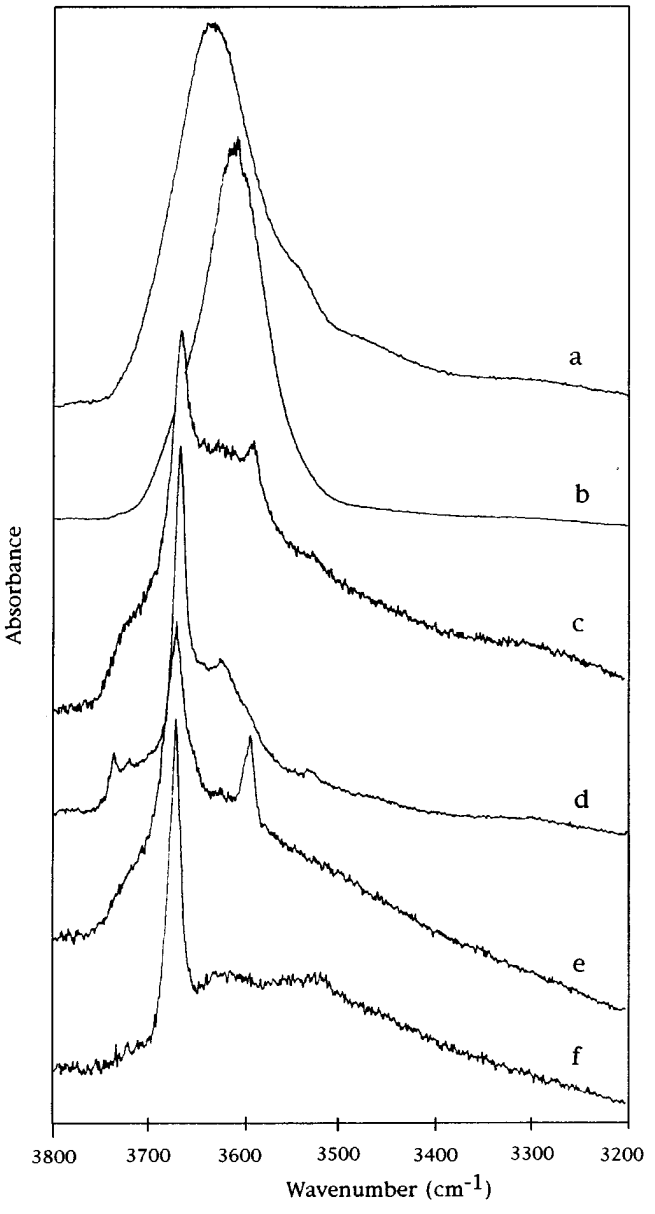

FIG. 1. Infrared spectra in the OH stretching region of dehydrated films of (a) AlP-SB; (b) SB; (c) AlP-EY; (d) EY; (e) AlP-SAPCA; (f) SAPCA.

of our films), which was assigned to some OH groups pointing to the exchangeable cations of the interlayer region.

In pillared saponites, a new OH band is clearly seen at 3595 cm^{-1}, more intense in AlP-SAPCA than in AlP-EY, and at the same wavenumber as the one previously reported by Chevalier *et al.* (15). The higher intensity for the former one may be related to its higher initial CEC. Such a band is not observed in the spectrum of pillared montmorillonite (AlP-SB). Pillared saponites also show a broad absorption between the two well-defined bands, probably associated with the different types of OH groups of interlayered Al species (25). Between pillared and unpillared SB, some

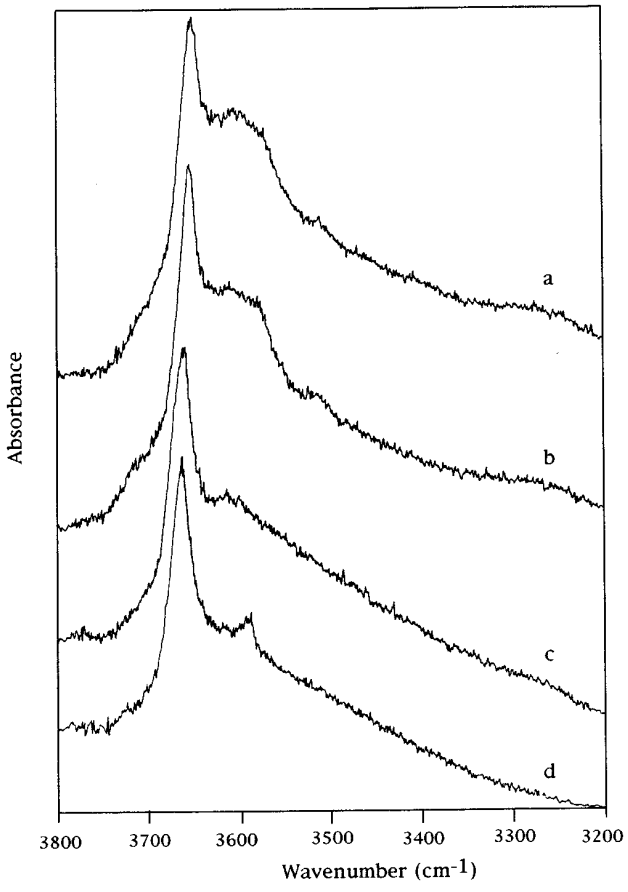

FIG. 2. Infrared spectra in the OH region of (a) AlP-EY after pyridine adsorption (room temp.) and outgassing at 150°C and (b) after outgassing at 300°C; (c) AlP-SAPCA after pyridine adsorption (room temp.) and outgassing at 150°C and (d) after outgassing at 300°C.

differences are noticed: broadening and shift by 30 cm^{-1} of the main absorption band towards higher wavenumbers and a shoulder showing up near 3560 cm^{-1}.

In the case of pillared saponites pyridine adsorption and subsequent outgassing results in the complete removal of the band at 3595 cm^{-1}, as shown in Fig. 2, which points to the acid nature of these OH groups. These observations are in agreement with those of the authors cited above. Outgassing pillared saponites at 300°C partially restores the band. No spectral modification upon pyridine adsorption could be observed in the stretching region in the case of pillared montmorillonite.

The spectra recorded in the region where pyridine in interaction with Brønsted and Lewis acid sites may be distinguished are shown in Fig. 3. Only the spectra recorded after outgassing at 300°C are given. The three pillared samples similarly contain both Lewis and Brønsted acid sites, as evidenced by the characteristic absorptions of pyridine near, respectively, 1450 and 1550 cm^{-1}. The two bands at 1490 and 1620 cm^{-1} are assigned to pyridine in interaction with both types of acid sites (25) and with H-bonded pyridine (15).

Catalytic Activity: Hydroconversion of Heptane

In a first set of experiments, it was checked that the reaction was not affected by the amount of metal (Pt) used. Indeed, in bifunctional catalysis, a good balance between the acid and metal functions has to be kept (26, 27). Samples of Al-pillared EY saponite were therefore impregnated with the required amounts of the platinum salt in order to load the solids with, respectively, 0.05, 0.2, 0.6, 1.0, and 1.5 wt% Pt. The catalytic tests were performed under the conditions mentioned in the Experimental section. The results are shown in Fig. 4.

The curves of total conversion of heptane versus temperature are not appreciably modified by the metal content (upper curves), slightly higher conversions being noticed with 1.5% Pt, and slightly lower ones for the sample with 0.05% Pt. With the highest Pt loading, the yields of isomers at maximum isomerisation conversion are slightly but significantly lower (central curves), whereas higher cracking yields are achieved (lower curves). In view of these results, the different catalysts were evaluated using a metal loading of 1 wt%.

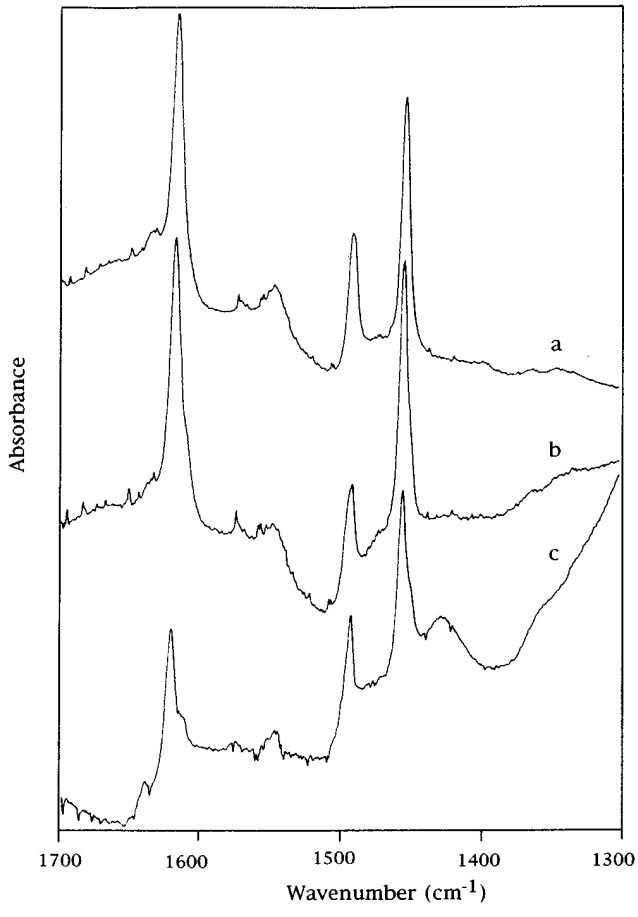

FIG. 3. IR spectra in the 1700–1300 cm^{-1} region after pyridine adsorption and subsequent outgassing at 300°C of (a) AlP-SAPCA; (b) AlP-EY; (c) AlP-SB.

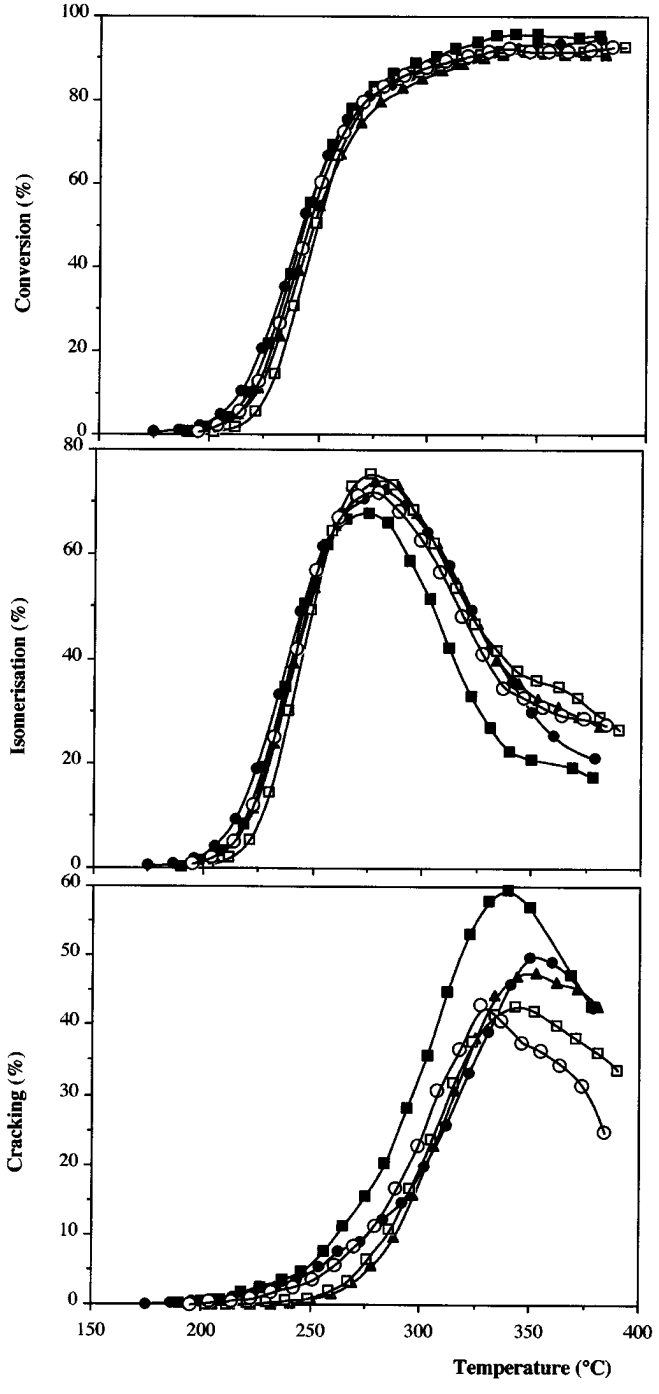

FIG. 4. Influence of the platinum loading on the reaction of heptane over AlP-EY: variation of total conversion (top figure), of the yield of C_7 isomers (central figure), and of the cracked products (bottom figure) vs reaction temperature. Metal loading (wt/wt%): ▲, 0.05; □, 0.2; ◯, 0.6; ●, 1.0; ■, 1.5.

The variation of the total conversion of heptane versus reaction temperature for the different Al-pillared clays prepared with the $\leq 2\ \mu$ fractions is shown in Fig. 5. Clearly, the catalytic performances of Al-pillared saponites are superior to those of Al-pillared montmorillonites. It should be mentioned that the results obtained over the Al-pillared montmorillonites are typical of the catalytic behavior of all montmorillonites so far investigated in this reaction, whatever their origin; none of those reached total conversion in this range of temperatures. These results are consistent with previous studies (3–7, 10), and seem to confirm that clays with tetrahedral lattice substitutions (saponites, beidellites) generate, upon Al-pillaring, catalysts which are substantially more active than clays with octahedral substitutions (montmorillonites, hectorites), at least in this type of proton-catalysed reactions. Noteworthy are the similar results obtained over the reference Ballarat saponite (AlP-SAPCA) and sample AlP-EY. For AlP-SC27, the conversion curve is translated toward higher temperatures. As seen earlier, this pillared sample has a lower content of pillar Al, a higher proportion of associated sepiolite, a poorer X-ray crystallinity (or stacking order) of the starting clay, and, as inferred from the larger half height peak width, less ordered interlayered pillars, although its acid content is similar to that of AlP-EY.

The variation of the yields of isomers of heptane versus conversion is shown in Fig. 6, where the diagonal indicates 100% selectivity. This figure is another illustration of the differences existing between the two types of pillared clays. Thus, Al-pillared saponites are not only more active than Al-pillared montmorillonites, but they also produce more isomers of heptane. Yields as high as 71% are obtained with Al-pillared EY (72% over AlP-SAPCA), a value which is higher than those obtained over Pt/H-dealuminated mordenites and dealuminated H-Y zeolites tested under identical experimental conditions (28). Figure 7 shows the variation of the proportion of mono-branched (2Me-C_6, 3Me-C_6,

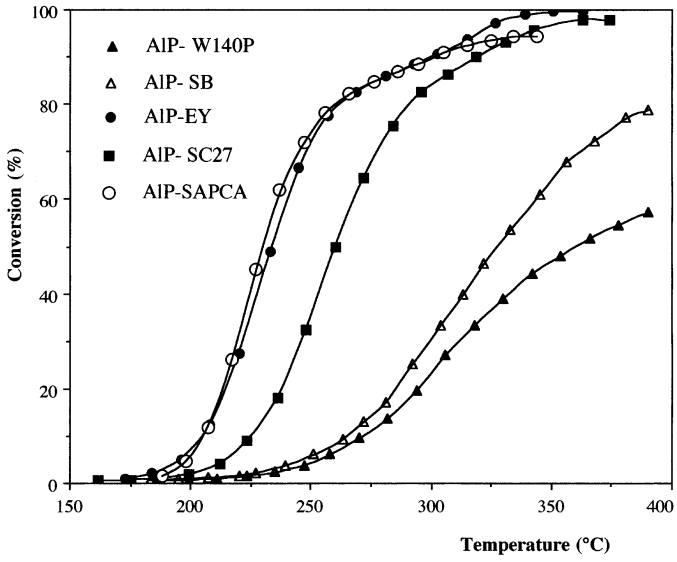

FIG. 5. Variation of heptane transformation vs reaction temperature over aluminium pillared clays: ▲, AlP-W140P; △, AlP-SB; ●, AlP-EY; ■, AlP-SC27; and ◯, AlP-SAPCA.

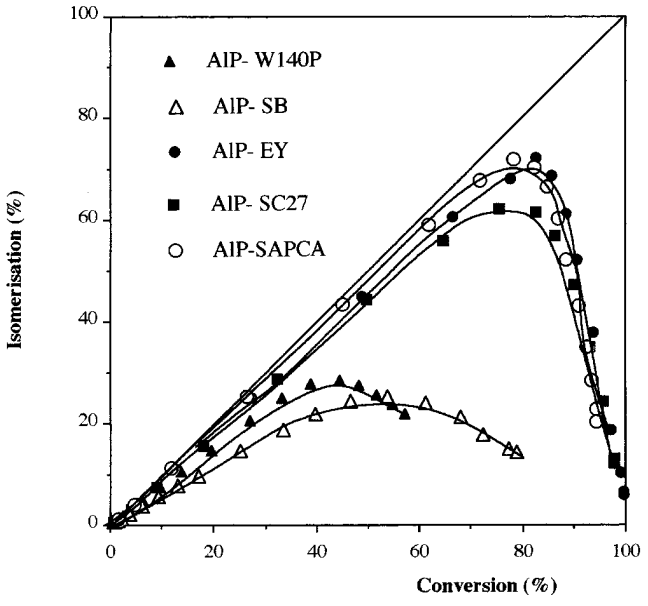

FIG. 6. Yields of C_7 isomers vs conversion of heptane (same symbols as in Fig. 5).

3Et-C_5) and dibranched isomers (2,3DMe-C_5, 2,4DMe-C_5, 2,2DMe-C_5, and 3,3DMe-C_5) versus the total conversion of heptane. The experimental values fall on the same curves, irrespective of the sample considered. It illustrates the consecutive character of the transformation of monobranched into dibranched isomers. Among the isomerisation products, 2Me-C_6 and 3Me-C_6 are the most abundant.

The apparent activation energies for the isomerisation reaction obtained from the Arrhenius plot (ln k vs $1/T$) were 128 and 131 kJ mol^{-1} for, respectively, AlP-EY and AlP-SC27, 84 kJ mol^{-1} for AlP-W140, and 87 kJ mol^{-1} for AlP-SB. Values of 135 and 109 kJ mol^{-1} have been recently reported by Campelo *et al.* (29) for the same reaction carried over Pt/SAPO-5 and Pt/SAPO-11, respectively, and between 125 and 140 kJ mol^{-1} over a series of Pt/H-Y dealuminated zeolites (30).

In order to establish whether the catalytic properties were influenced by the particle size of the starting clays, the reaction has been carried out over pillared materials prepared with the raw clays and the results have been compared with those obtained over the $<2\ \mu$ pillared samples. For the three saponites, the differences observed were trivial, the yields of isomers at maximum isomerisation being almost identical and therefore independent of the clay particle size (see also Table 6). However, in the case of AlP-SB, a marked enhancement of the isomerisation conversion was noticed for the sample prepared from the unrefined clay. Indeed, the yield of isomers at maximum isomerisation conversion was 34.1% instead of 25.4% for the $<2\ \mu$ fraction pillared under identical conditions. A similar observation was also made in the case of AlP-W140, although it is less marked.

DISCUSSION

The characterisation data of Tables 2 to 4 indicate that the main structural and textural criteria generally considered to assess suitable pillaring of smectites are met. Indeed, spacings of about 18 Å (pillar heights of about 9 Å), surface areas of the order of 200 m^2/g or higher, and micropore volumes of about 0.050 cm^3/g or higher are obtained for the precursors (uncalcined samples) as well as for the calcined samples. It has also been shown that pillaring the raw clay or the small fractions ($<2\ \mu$) has no marked influence on the *d* spacings (pillar or gallery height), but results in increased amounts of pillar Al (lower residual CEC) which, for pillared SC27 and EY saponites, may represent a relative gain of, respectively, 27 and 35%. However, the improvement of the degree of occupancy of the interlayer region by Al species for these two clays may be only partly real since usually the contamination phase(s), in the present case sepiolite, are relatively more concentrated in the crude clay samples. Note that the two montmorillonites, where no contamination phase could be evidenced by X-ray diffraction, also show, although to a lesser extent, lower residual CEC values for the pillared samples obtained with the raw fraction. From the data of Table 3, the fractions of the charge neutralised by Al species may be estimated. For the series prepared with the $<2\ \mu$m fractions, the values 0.56, 0.62, 0.49, and 0.43 are obtained for, respectively, AlP-W140, AlP-SB, AlP-SC27, and AlP-EY, namely higher relative Al content (as pillars) for the two montmorillonites. Those prepared with the raw clays are, in the same sequence, 0.61, 0.64, 0.62, and 0.63. Apparently, pillaring raw clays seems preferable as the pillar density is improved, which is consistent with the slightly improved *d* spacings and thermal resistance of the pillars.

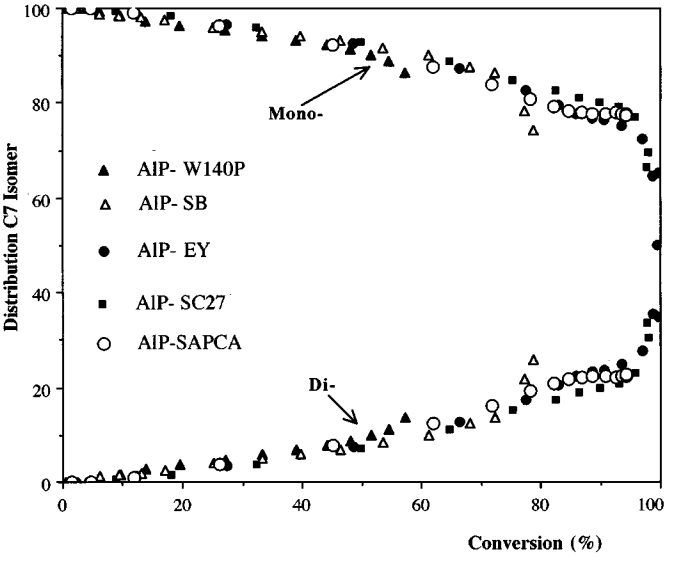

FIG. 7. Variation of the monobranched and dibranched C_7 isomers vs conversion of heptane (same symbols as in Fig. 5).

TABLE 6

Comparative Data for Hydroconversion of Heptane Obtained at Maximum Isomerisation Conversion

Samples	T Max Iso (°C)	Conv. (%)	Y Iso (%)	Y Cra. (%)	Y Cycl. (%)	Sel. Iso (%)
Montmorillonite						
AlP-W140P[a]	342	44.3	28.5	10.2	5.6	64.3
AlP-W140P[b] (RT)	335	54.3	31.4	17.0	5.9	44.2
AlP-W140P[b] (60°C)	341	60.9	26.9	25.1	8.9	47.3
AlP-SB[a]	333	53.7	25.4	21.5	6.8	47.3
AlP-SB[b]	326	61.8	40.3	17.0	4.5	65.2
AlP-WL[a]	330	53.3	26.8	16.9	9.6	50.4
AZA[a]	346	62.0	45.0	15.0	2.0	74.0
FAZA[a]	346	56.0	39.0	16.0	1.0	69.0
AlP-N4[a]	331	67.4	40.7	24.9	1.8	60.4
AlP-N7[a]	309	79.8	57.9	18.8	3.1	72.6
AlP-Beidellite	280	83.2	61.7	20.9	0.6	74.2
Saponites						
AlP-SC27[a]	284	75.4	62.2	12.5	0.7	82.5
AlP-SC27[b]	288	81.8	62.3	18.0	1.5	76.2
AlP-EY[a]	269	82.9	70.8	12.1	0.0	85.4
AlP-EY[b]	268	80.3	69.5	10.8	0.0	86.5
AlP-SAPCA[a]	257	83.5	71.8	11.7	0.0	86.0
AlP-SAPCA[b]	256	78.2	71.9	6.3	0.0	91.9
Zeolites						
H-Mordenite	229	71.9	59.0	13.0	0.0	82.0
H-Y 82	221	80.0	60.4	19.6	0.0	75.5
H-Y-CBV-600	237	77.1	63.9	13.2	0.0	83.0

[a] 2 μ fraction.
[b] Raw clay.

The acid contents determined by adsorption–desorption of ammonia show important differences among the various pillared clays, with a factor greater than 2 between the least (AlP-W140) and the most acidic samples (AlP-SAPCA). Such differences are reflected neither in the textural nor in the structural properties of the corresponding samples. They are consistent with their respective catalytic activities.

For the sake of comparison, catalytic results obtained over the pillared materials under investigation and over a few other Al-pillared clays and zeolites (see the Experimental section) have been compiled in Table 6. The different columns refer, respectively, to the temperature at which isomerisation conversion is a maximum (Tmax Iso), the corresponding total conversion of heptane, the yields of isomers (Yiso), cracked (Ycr), and cyclised (Ycyc) products, and the selectivity to the C7 isomers (Sel.). Samples AlP-W140P(RT) and AlP-W140P(60) refer to materials which were pillared with a solution having an OH/Al molar ratio of 2.4 instead of 1.6, the final suspension being aged at room temperature (RT) and at 60°C, respectively.

In terms of activity, the zeolites are more active than the pillared clays, with temperatures at maximum isomerisation conversion substantially lower than for any of the clay-based catalysts. This is probably to be related to the higher strength of the protonic sites in zeolites. In terms of yields and selectivities to isomers of heptane, the pillared saponites are as efficient or even superior to the zeolites, according to the type of zeolite considered. It should be noted that the data reported for H-Y CBV 600 were the best ones obtained over a series of seven commercial dealuminated samples, with Si/Al ratios ranging between 2.6 and 37 (30). For mordenite, the data were selected out of a series of 34 different dealuminated samples (23). On the contrary, the Al-pillared montmorillonites (W-140P, SB, WL, AZA, FAZA), independently of the origin of the clay, are the least active catalysts as regards Tmax Iso, total conversion, and selectivity to C7 isomers. They also have lower acid contents. Al-pillared beidellite, another clay with tetrahedral Si for Al substitutions, exhibits catalytic performances similar to those of the saponites (high conversions and high yields of isomers), whereas for Al-pillared clays with intermediate levels of tetrahedral substitutions (AlP-N4 and AlP-N7) (9), the catalytic results are situated between those of pillared saponites and montmorillonites. Higher activity of Al-pillared beidellite with respect to Al-pillared montmorillonite was also observed in the alkylation of biphenyl with propylene (31) and dehydration of 2-propanol (32). Note that the montmorillonite pillared with a solution with OH/Al molar ratio of 2.4 (sample AlP-W140P(TA) instead of 1.6 (sample AlP-W140P), shows improved catalytic

properties. However, total conversion of heptane does not exceed 70% over Al-pillared montmorillonites, as observed in previous works (3–8). The relatively higher cracking yields obtained over pillared montmorillonites are partly due to hydrogenolysis occurring over the metal function, as revealed by the proportion of butane in the cracking products (instead of iso-butane, which is produced from the C7 isomers), therefore pointing to a somewhat poorer balance of the two functions. Table 6 also shows that, parallel to the increasing efficiency of the different pillared materials, the yields of cyclisation products (benzene and mainly toluene) diminish. As for zeolites, those products are not formed over the best pillared saponites.

The higher activity and acid content of Al-pillared saponites compared with Al-pillared montmorillonites (Table 5) cannot be accounted for either by their textural characteristics or by differences in the number of pillars. Indeed, both types of pillared materials exhibit similar spacings (or gallery heights) after calcination at 400°C and, except for sample AlP-SC27, a similar content of pillar Al (Table 3). Moreover, if the micropore volume was a determining factor, AlP-SB with a higher micropore volume (after calcination at 400°C) and also a greater amount of pillar Al (see Table 3) than the two pillared saponites (AlP-EY, AlP-SC27) should exhibit higher performance.

If the catalytic activity was only related to the acid content determined by ammonia adsorption–desorption, one would expect the yields of isomers over AlP-SB, with intermediate acid content, to be somewhere between pillared montmorillonites and pillared saponites, which is not the case.

It has been shown in previous studies (3, 4, 10) that in beidellites (clay with tetrahedral lattice substitutions), proton attack of tetrahedral Si–O–Al linkages generate Si–OH . . . Al groups exposed at the surface of the solids and characterised by an IR OH stretching band at 3440 cm^{-1}. This band was observed in H-exchanged beidellite, upon decationation of ammonium exchanged samples, as well as in the Al-pillared forms. These silanol groups were thermally stable (IR band still visible after calcination at 600°C in vacuo), and acidic (the band disappeared upon adsorption of pyridine, and the band characteristic of pyridinium ions showed up at 1545 cm^{-1}). Similar groups have been observed recently by Chevalier *et al.* (15) in Al-pillared or H-exchanged Ballarat saponite, as well as in this study; the main difference with beidellite is that in saponites, the OH vibration appears at 3594 cm^{-1}. The acid character of these new OHs has been shown by pyridine adsorption experiments, confirming the observation of the authors cited above.

In montmorillonites, most of the substitutions occur within the octahedral layers, tetrahedral substitutions being in rather limited amounts and, consequently, such groups are not shown by infrared spectroscopy. The exact nature of the Brønsted acid sites in Al-pillared montmorillonites is still controversial. Some authors (including ourselves) assume that, in these clays, the protons accompanying the pillaring process and those resulting from the transformation of the pillar precursors (hydrated Al species) into the anhydrous pillars (oxide form) migrate with increasing temperature toward the octahedral layers (33), probably through a Hofmann–Klemen type effect (34), as in heat-treated Li-exchanged clays. This migration (partly reversible since ammonium ions are formed upon adsorption of ammonia (35)) could account both for the lower thermal stability and catalytic activity, as has been shown previously (3). Several authors also observed the disappearance of the pyridinium IR band (Brønsted sites) at outgassing temperatures as low as 300–400°C (36–39). In a recent study, Fetter *et al.* (40) associated the strong acidity of Al-pillared montmorillonites with the tetrahedral aluminium present in the pillars. Although the contribution of pillar tetrahedral Al may be real, it does not allow one to account for the significant discrepancies found between the two types of clays as regards their respective acid contents and catalytic activities, which, as stated earlier, are not reflected in the structural and textural characteristics, as well as by the amounts of pillar Al.

The interpretation summarised above was invoked in previous work to account for the catalytic results obtained over Al-pillared montmorillonites and beidellites, in particular in the hydroconversion of decane (9) and, recently, of heptadecane (41), where a similar clear distinction between the two types of clays has been clearly observed. From the data reported in this study, and the similar catalytic behavior of Al-pillared saponites and beidellites, the important differences in activity and activation energies found between Al-pillared montmorillonites (mean value of 85 kJ/mol) and saponites (mean value of 130 kJ/mol) may be accounted for by the presence, in Al-pillared saponites, of stronger Si–OH . . . Al catalytic sites, which is also in agreement with Corma *et al.* (42).

The reaction mechanism has not been addressed in this study. In a recent article on the reaction of heptane over Pd/H-beta zeolite, Blomsma *et al.* (43) have shown that the classical bifunctional mechanism for isomerisation and hydrocracking could not account for the detailed examination of the reaction products without introducing a fast dimerisation-cracking pathway. As the reaction products obtained over the two types of pillared clays (more particularly over pillared saponites) are identical to those found over H-zeolites, it seems that such a mechanism might also operate in the case of Al-pillared clays. This point will be treated in more detail in a separate article. Finally, the apparent activation energies established for the two varieties of pillared clays (with mean values of 130 kJ for the pillared saponites, and 85 kJ for the pillared montmorillonites) are also consistent, as discussed by Corma et al. (43), with differences in the strength of the acid sites.

CONCLUSION

Al-pillaring of montmorillonites and saponites results in thermally stable 17–18 Å expanded solids presenting similar structural and textural characteristics and Al amounts involved as pillars, but different acid contents.

The catalytic results of heptane hydroconversion obtained over Pt-impregnated Al-pillared montmorillonites and saponites prepared under similar conditions show that Al-pillared saponites are more efficient isomerisation catalysts than Al-pillared montmorillonites, and at least as performing as dealuminated acid mordenites and commercial Y-zeolites. The superior catalytic performances of the pillared saponites with respect to those of Al-pillared montmorillonites is attributed, as in the case of Al-pillared beidellites, to the presence of stronger Si–OH . . . Al acid sites, which only occur in smectites where lattice substitutions are mainly located within the tetrahedral layers. In montmorillonites, these substitutions take place principally in the octahedral layers and, therefore, sites with equivalent strength are absent.

ACKNOWLEDGMENT

This work is part of a research programme sponsored by EEC (BRE2-CT94-0629).

REFERENCES

1. Mokaya, R., and Jones, W., *J. Chem. Soc. Chem. Commun.* 929 (1994).
2. Mokaya, R., and Jones, W., *J. Catal.* **153**, 76 (1995).
3. Poncelet, G., and Schutz, A., *in* "Chemical Reactions in Organic and Inorganic Constrained Systems" (R. Setton, Ed.), p. 145. Reidel, Dordrecht, 1986.
4. Schutz, A., Plée, D., Borg, F., Jacobs, P. A., Poncelet, G., and Fripiat, J. J., *in* "Proceedings, Int. Clay Conf., Denver" (L. G. Schultz, H. van Olphen, and F. A. Mumpton, Eds.), p. 303. Clay Mineral Soc. 1987.
5. Molina, R., Schutz, A., and Poncelet, G., *J. Catal.* **145**, 79 (1994).
6. Plée, D., Schutz, A., Poncelet, G., and Fripiat, J. J., *in* "Catalysis by Acids and Bases" (B. Imelik *et al.*, Eds.), p. 343. Elsevier Sci. Amsterdam/New York, 1985.
7. Vieira-Coelho, A., and Poncelet, G., *in* "Pillared Layered Structures" (I. V. Mitchell, Ed.), p. 185. Elsevier Appl. Sci., Amsterdam, 1990.
8. Vieira-Coelho, A., and Poncelet, G., *Appl. Catal.* **96**, 2614 (1991).
9. Molina, R., Moreno, S., Vieira-Coelho, A., Martens, J. A., Jacobs, P. A., and Poncelet, G., *J. Catal.* **148**, 304 (1994).
10. Schutz, A., Stone, W. E. E., Poncelet, G., and Fripiat, J. J., *Clays Clay Miner.* **35**, 251 (1987).
11. Butruille, J. R., and Pinnavaia, T. J., *Catal. Today* **14**, 141 (1992).
12. Jiang, D. Z., Sun, T., Liu, Z. Y., and He, M. Y., *in* "Proceedings, 9th Int. Zeolite Conf." (R. Von Ballmoos, J. B. Higgins, and M. M. J. Tracey, Eds.), Vol. 2, p. 631. Butterworth-Heinemann, Boston, 1993.
13. Schoonheydt, R. A., van den Eynde, J., Tubbax, H., Leeman, H., Stuyckens, M., Lenotte, I., and Stone, W. E. E., *Clays Clay Miner.* **41**, 598 (1993).
14. Chevalier, S., Suquet, H., Franck, R., Marcilly, C., and Barthomeuf, D., *in* "Expanded Clays and Other Microporous Solids" (M. L. Occelli and H. Robson, Eds.), p. 32. Van Nostrand–Reinhold, New York, 1992.
15. Chevalier, S., Franck, R., Seuquet, H., Lambert, J. F., and Barthomeuf, D., *J. Chem. Soc. Faraday Trans.* **90**(4), 667 (1994).
16. Lambert, J. F., Chevalier, S., Franck, R., Suquet, H., and Barthomeuf, D., *J. Chem. Soc. Faraday Trans.* **90**(4), 675 (1994).
17. Chevalier, S., Franck, R., Lambert, J. F., Barthomeuf, D., and Suquet, H., *Appl. Catal.* **110**, 153 (1994).
18. Post, J. L., *Clays Clay Miner.* **32**, 147 (1984).
19. Michot, L. J., and Pinnavaia, T. J., *Chem. Mater.* **4**, 518 (1992).
20. Remy, M. J., and Poncelet, G., *Microporous Mater.*, in press.
21. Dietz, W. A., *J. Gas Chromatogr.* 70 (1967).
22. Kaloidas, V., Koufopanos, C. A., Gangas, N. H., and Papayannakos, N. G., *Microporous Mater.* 97 (1995).
23. Moreno, S., and Poncelet, G., article in preparation.
24. Casal, B., Merino, J., Ruiz-Hitzky, E., Gutierrez, E., and Alvarez, A., *Clay Miner.*, in press.
25. Bodoardo, S., Figueras, F., and Garrone, E., *J. Catal.* **147**, 223 (1994).
26. Weitkamp, J., *in* "Hydrocracking-Hydrotreating" (J. Ward and S. A. Quader, Eds.), ACS Symposium Series, Vol. 20, p. 1. Am. Chem. Soc., Washington, DC, 1975.
27. Martens, J., and Jacobs, P. A., *in* "Theoretical Aspects of Heterogeneous Catalysis" (J. B. Moffat, Ed.), p. 52. Van Nostrand–Reinhold, New York, 1990.
28. Remy, M., Moreno, S., and Poncelet, G., in preparation.
29. Campelo, J. M., Lafont, F., and Marinas, J. M., *J. Catal.* **156**, 11 (1995).
30. Remy, M. J., Stanica, D., Poncelet, G., Feijen, E. J. P., Grobet, P. J., Martens, J. A., and Jacobs, P. A., *J. Phys. Chem.* in press.
31. Butruille, J. R., Michot, L. J., Barres, O., and Pinnavaia, T. J., *J. Catal.* **129**, 664 (1993).
32. Urabe, K., Kouno, N., Sakurai, H., and Izumi, Y., *Adv. Mater.* **3**(11), 558 (1991).
33. Auer, H., and Hofmann, H., *Appl. Catal.* **97**, 23 (1993).
34. Hofmann, U., and Klemen, R., *Z. Anorg. Chem.* **262**, 95 (1950).
35. Vaughan, D. E. W., Lussier, R. J., and Magee, J. S., U.S. Patent 4,271,043 (1981).
36. Occelli, M. L., and Lester, J. E., *Indus. Eng. Chem. Prod. R&D* **24**, 27 (1985).
37. Tichit, D., Fajula, F., Figueras, F., Gueguen, C., and Bousquet, J., *in* "Fluid Cracking Catalysts" (M. L. Occelli, Ed.), ACS Symposium Series, Vol. 375, p. 237. Amer. Chem. Soc., Washington, DC, 1988.
38. Ko, A.-N., and Chang, H.-C., *J. Chin. Chem. Soc.* **39**, 81 (1992).
39. Bradley, S., and Kidd, R. A., *J. Catal.* **141**, 239 (1993).
40. Fetter, G., Tichit, D., de Menorval, L. C., and Figueras, F., *Appl. Catal.* **126**, 165 (1995).
41. Martens, J., Coelho-Vieira, A., Jacobs, P. A., and Poncelet, G., in preparation.
42. Corma, A., Llopis, F., Monton, J. B., and Weller, S., *J. Catal.* **142**, 97 (1993).
43. Blomsma, E., Martens, J. A., Jacobs, P. A., *J. Catal.* **155**, 141 (1995).